

Difference Sphere: An Approach to Near Light Source Estimation

Takeshi Takai, Atsuto Maki, Koichiro Niinuma, Takashi Matsuyama

*Graduate School of Informatics, Kyoto University, Yoshida-Honmachi, Sakyo-ku,
Kyoto 606-8501, Japan.*

Abstract

We present a novel approach for estimating light sources from a single image of a scene that is illuminated by major near point light sources, a few directional light sources and ambient light. We propose to employ a pair of reference spheres as light probes and introduce the difference sphere that we acquire by differencing the intensities of two image regions of the reference spheres. Because the effect by directional light sources and ambient light is eliminated by differencing, the key advantage of considering the difference sphere is that it enables us to identify near point light sources including their radiant intensities. We also show that analysis of gray level contours on spherical surfaces facilitates separate identification of multiple combined light sources and is well suited to the difference sphere. We demonstrate the effectiveness of the entire algorithm with experimental results while also investigating the applicability to an open scanner in indoor scene.

Key words: Difference sphere, inverse lighting, near light source, contour representation, open scanner

PACS:

1 Introduction

Acquiring the knowledge of light sources is crucial in computer vision as well as in computer graphics especially with the recent advent of image based rendering techniques. Once the parameters of light sources are obtained, the illumination information can be effectively utilized for manipulating shadows, highlights, or shading on real/virtual object in images. In this paper, we consider the problem of estimating several co-existing light sources from a single image using a pair of spheres whose surface has Lambertian property. In particular, we deal with major near point light sources, besides directional light source and ambient light, so that the reality of manipulated images should be increased.

The problem of estimating illuminant directions arises in the context of shape from shading [1] and early work focused on recovering a single distant light source assuming Lambertian surface and uniform albedo of target object. See [2,3] for a few example. Since, there have been successful attempts to recover a more general illumination description [4]. Marschner and Greenberg [5] propose a method for estimating directions and radiant intensities of a few light sources in a scene by a least-squares method for surface intensity functions. In [6], Yang and Yuille also solve for a small number of light sources by exploiting the constraints by occluding boundary. As an extension, Zhang and Yang [7] introduce a technique for estimating directions and radiant intensities of multiple light sources. While they analyze a single image of a reference sphere with known shape and Lambertian reflectance model, Zhou and Kambhamettu [8] extract these properties using stereo images of a reference sphere with specular reflection. They estimate the directions by the positions of highlights and radiant intensities from shading. Also, Maki [9] utilizes multiple images of an object that is in motion for estimating the illuminant direction by observing the brightness variance derived on the object surface. In [10], Miyazaki et al. utilize single viewed object and determine the illumination directions from the position of the brightest intensity in the specular component whereas they compute surface normal of the object by shape-from-polarization. Also, Hara et al. [11] employ a single view image of an object and its geometric model and estimate the direction and intensity of multiple light sources as well as the specular reflectance property of the object using an EM optimization framework. However, none of these approaches have made account for near point light sources that have varying effect depending on the distance.

Debevec [12] uses a mirrored ball as a light probe for measuring an entire radiance distribution of real scene. Another efficient method is that of Sato et al. [13], which explicitly measures the 3D lighting distribution of the upper hemisphere using a stereo omni-directional image that is captured with a fish-eye lens. They have also developed a smart method [14] of estimating the illumination distribution by exploiting information of a radiance distribution inside shadows cast by an object of known shape. Cast shadows were also utilized by Cao and Foroosh [25] for computing the orientation of solar light. While the effectiveness of these approaches has been shown for global illumination, they are essentially for estimating distant lighting. Thus, regarding near light sources, further accurate characterization of lighting is desired.

Powell et al. [15] present a technique for calibrating the light source geometry by matching highlights on three spheres. Zhou and Kambhamettu [16] also design a scheme for estimating the size and location of multiple area light sources by extending their work [8] of using a sphere with a specular surface. With these geometric matching methods, the positions of light sources are available, but not their radiant intensity.

In this paper we propose a novel method for estimating parameters of light sources¹, i.e., ambient light, directional light sources, and in particular near point light sources including their radiant intensity which is necessary for certain applications such as an open scanner. Assuming indoor scenes where direct near light sources are more influential than indirect lighting, we employ a pair of reference spheres as a light probe and analyze gray level contours on the spherical surfaces so that 3D geometric and photometric properties of the direct light sources can be explicitly characterized. Our key idea then is in introducing the notion of *difference sphere* that we acquire by differencing two image regions of the reference spheres. We show that separate identification of multiple combined light sources is facilitated through an analysis of gray level contours on the difference sphere.

The sequel of the paper is composed as following. In Section 2 we define the lighting and reflectance model. While introducing the notion of difference sphere, we discuss about the characteristics of single and difference sphere in Section 3. Section 4 provides the description of our algorithm of light source estimation followed by evaluations of our proposed method in Section 5. Finally we conclude the paper with discussions in Section 6.

2 Model Definitions

2.1 Assumptions

For our light source estimation we employ a pair of spheres with known size, which we call *reference spheres*, and assume a bidirectional reflectance distribution function as Lambertian. Figure 1 illustrates an example of a configuration for our light source estimation. We place the spheres in a way that they do not occlude or cast shadows to each other. We also assume that the camera for capturing images and the reference spheres are accurately calibrated. We then deal with measured image irradiance which we in this paper refer to as image intensity. In other words, ignoring camera gain, we assume that the transformation function from the radiance to the pixel gray value is spatially uniform and linear with zero bias so that the scale factor is equal to 1. We consider the possible diffuse-interreflection in the scene as minor and behaves as ambient light.

¹ The content of this article has partly appeared in [23].

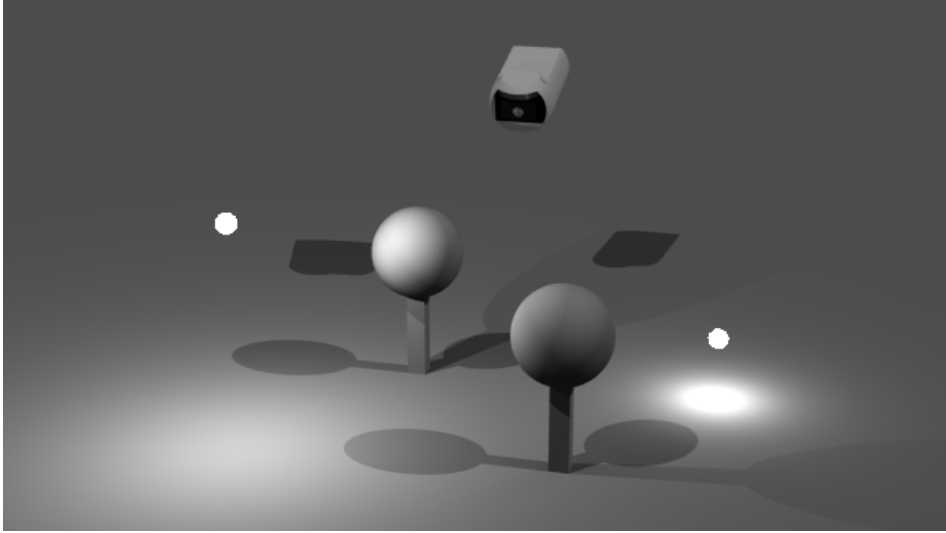


Fig. 1. Example of a configuration for our light source estimation

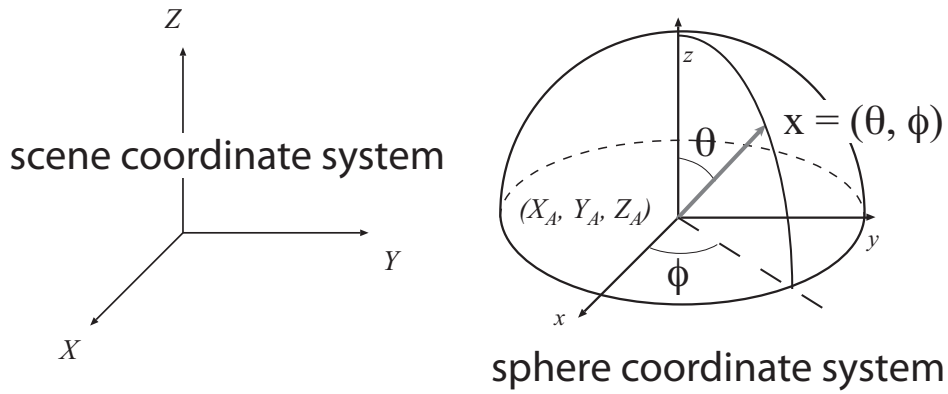


Fig. 2. Coordinate systems

2.2 Coordinate Systems

As illustrated in Figure 2 we consider the *scene coordinate system* (X, Y, Z) and the *sphere coordinate system* (x, y, z) . Given a reference sphere, A , we align each axis of the sphere coordinate system, x_A , y_A , and z_A , parallel to X , Y , and Z axis of the scene coordinate system, respectively. We also utilize the *surface coordinate system* (θ, ϕ) in order to specify angular positions of spherical surface points.

2.3 Light Sources

We deal with radiance due to three types of light sources which we describe below, denoting the reflectance coefficient of the reference sphere as η .

- **Near point light:** At point \mathbf{X} on the surface of reference sphere, let $\alpha_p(\mathbf{X}, \mathbf{P})$ be the angle between the surface normal and the line from the light source whose position is \mathbf{P} . The radiance, $I_p(\mathbf{X}; \mathbf{P})$, is then given by²

$$I_p(\mathbf{X}; \mathbf{P}) = \eta L_p \cos \alpha_p(\mathbf{X}, \mathbf{P}) / d(\mathbf{X}, \mathbf{P})^2, \quad (1)$$

where L_p denotes radiant intensity of the point light source, and $d(\mathbf{X}, \mathbf{P})$ the distance between the light source and \mathbf{X} .

- **Directional light:** Let $\alpha_d(\mathbf{X})$ be an angle between the surface normal at point \mathbf{X} and the direction of the light source. With the radiant intensity of the directional light source, L_d , the radiance, $I_d(\mathbf{X})$, is given by

$$I_d(\mathbf{X}) = \eta L_d \cos \alpha_d(\mathbf{X}). \quad (2)$$

- **Ambient light:** It provides constant light for a scene. We consider it as bias in this paper. If the scene were illuminated by ambient light L_a alone, the radiance, I_a , of the reference sphere would simply be $I_a = \eta L_a$.

2.4 Radiance

The total radiance considering above can be modeled as

$$I(\mathbf{X}) = \sum_{i=1}^s I_p^{[i]}(\mathbf{X}; \mathbf{P}[i]) + \sum_{j=1}^t I_d^{[j]}(\mathbf{X}) + I_a, \quad (3)$$

where s and t are (unknown) numbers of point light sources and directional light sources, respectively, i and j are indexes of them, and $\mathbf{P}[i]$ is the 3D position of the i -th point light source in the scene coordinate system.

3 Characteristics of Single Sphere and Difference Sphere

In order to facilitate separate identification of multiple combined light sources, in this section, we introduce the notion of ***difference sphere***, which we acquire by differencing two image regions of reference spheres. We use the term, ***single sphere***, in place of reference sphere to explicitly distinguish it from difference sphere. In the following we assume perspective camera projection, and describe the characteristics of the single sphere and the difference sphere in detail.

² In the case $\cos \alpha_p(\mathbf{X}, \mathbf{P}) < 0$, the light source illuminates the point from behind, and thus the radiance equals 0. In the following descriptions, we consider the case of $\cos \alpha \geq 0$.

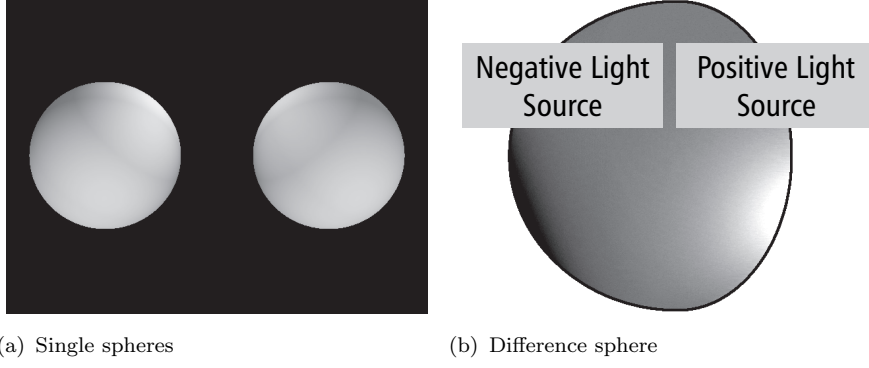


Fig. 3. Single spheres and difference sphere. The gray-level of (b) shows the radiance of the difference sphere; the bright/dark area reflects positive/negative values. The intensities of the image are emphasized for display reason.

3.1 Radiance

3.1.1 Single Sphere

Let us first consider a single sphere, A , with shading in a scene and formulate the radiance on the surface of the sphere in the sphere coordinate system.

Let \mathbf{x}_A represent a point on the surface of single sphere A , and $\mathcal{F}_A(\mathbf{x}_A)$ the 3D position of \mathbf{x}_A in the scene coordinate system. Representing the radiance, $I(\mathbf{X})$, in equation (3) by $I_A(\mathbf{x}_A)$, and thus replacing \mathbf{X} with $\mathcal{F}(\mathbf{x}_A)$, the constituents of it are given by

$$I_p^{[i]} = \eta_A L_p^{[i]} \cos \alpha_p^{[i]}(\mathcal{F}_A(\mathbf{x}_A), \mathbf{P}^{[i]}) / (D(\mathcal{F}_A(\mathbf{x}_A), \mathbf{P}^{[i]}))^2, \quad (4)$$

$$I_d^{[j]} = \eta_A L_d^{[j]} \cos \alpha_d^{[j]}(\mathcal{F}_A(\mathbf{x}_A)), \quad (5)$$

$$I_a = \eta_A L_a, \quad (6)$$

where η_A is the diffuse coefficient, and $L_p^{[i]}$ and $L_d^{[j]}$ denote the radiant intensity of the i -th point light source and the j -th directional light source, respectively. Note that both $\cos \alpha_p$ and $\cos \alpha_d$ accompany an index of light source accordingly.

3.1.2 Difference Sphere

We virtually generate a difference sphere, “ $A - B$ ”, from a pair of single spheres, A and B , that has the following properties. The location and the radius of it is inherited from those of single sphere A . Namely, the size of the spheres are normalized to that of single sphere A .

Let $I_A(\theta, \phi)$ and $I_B(\theta, \phi)$ denote the radiance of single spheres, A and B , respectively. The radiance of difference sphere, $A - B$, is ³

$$I_{A-B}(\theta, \phi) = I_A(\theta, \phi) - I_B(\theta, \phi). \quad (7)$$

From equations (3) - (6) and (7) the radiance, $I_{A-B}(\mathbf{x}_{A-B})$, at point \mathbf{x}_{A-B} on the surface of difference sphere $A - B$ is defined as follows:

$$\begin{aligned} I_{A-B}(\mathbf{x}_{A-B}) &= I_A(\mathbf{x}_A) - I_B(\mathbf{x}_B) \\ &= \sum_{i=1}^s I_p^{[i]}(\mathcal{F}_A(\mathbf{x}_A); \mathbf{P}[i]) - \sum_{i=1}^s I_p^{[i]}(\mathcal{F}_B(\mathbf{x}_B); \mathbf{P}[i]) \end{aligned} \quad (8)$$

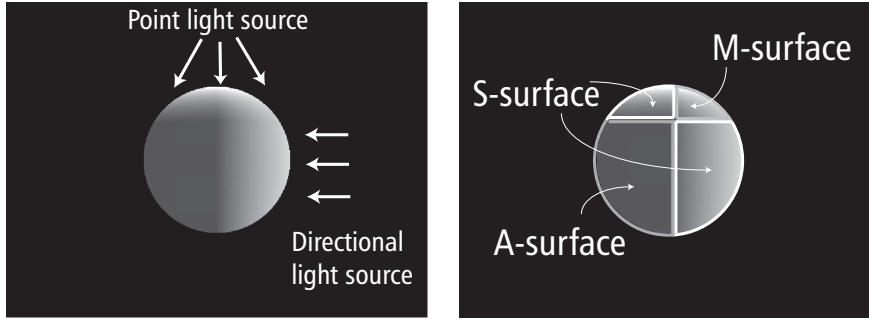
where surface coordinates of \mathbf{x}_{A-B} , \mathbf{x}_A , and \mathbf{x}_B on their corresponding spheres are all equivalent. Equation (8) is due to the fact that the differencing operation in equation (7) eliminates lighting effects caused by all the directional light sources and ambient light. That is, the illumination on a difference sphere is caused only by point light sources.

Further, since the differencing operation generally gives rise to negative radiance as well as positive ones, we could interpret the surface radiance of a difference sphere as if they were independently generated by *positive* and *negative* point light sources. Thus, a difference sphere is virtually illuminated by *positive* and *negative* point light sources, each of which introduces positive and negative radiance.

Figure 3 illustrates a difference sphere that is generated by a pair of single spheres, and show the positive and the negative radiance. In the subsequent analysis of surface radiance for estimating point light sources, negative radiance can be treated just equally as positive radiance without a loss of generality. Moreover, it turns out that we only need to analyze either positive radiance or negative one for estimating the point light sources since the influence of the light sources basically appear in both of them⁴. It is in general sensible to choose the radiance that represents larger amount of radiant energy.

³ Note that in the shading analysis that is described later, $I_{A-B}(\theta, \phi)$ becomes undefined for those (θ, ϕ) where the corresponding surface points on single spheres A or B cannot be observed by a camera.

⁴ However, note that the acquired lighting parameters in case of analyzing negative radiance should be interpreted in the coordinate system whose origin is at the center of single sphere B , instead of sphere A .



(a) A reference sphere under light sources (b) Divided surfaces

Fig. 4. Surface classification

3.2 Surface Analysis

Let us investigate the characteristics of the sphere surface while separating it into three categories depending on the types of illuminating light sources (see Figure 4). They are,

- **S-surface**: Illuminated by a single light source (and the ambient light). In particular, we call S -surface that is illuminated by a single point light source **S_p -surface** and that by a single directional light source **S_d -surface**.
- **M-surface**: Illuminated by multiple point and/or directional light sources.
- **A-surface**: Illuminated by ambient light alone.

Now, we focus on the characteristics of S -surface in order to estimate parameters of light sources. The notions of **feature plane** and **radiance ratio** play the important role:

- **Feature plane**: A set of points on S -surface with identical radiance forms an arc on a plane in 3D scene. We call the plane feature plane. The surface normal of the feature plane indicates the direction of the point/directional light source which illuminates the S -surface.
- **Radiance ratio**: The radiance ratio of a group of feature planes in an identical S -surface characterizes the radiant intensity of the light source.

In the remainder of the section, preceded by the analyses in the cases of a single point light source and a single directional light source which show the mechanisms of our light source estimation, we derive how the difference sphere simplifies the procedure of light source estimation. Note that we additionally define \mathbf{O} , the center of a reference sphere, \mathbf{l} , the direction of the light source, and r , the radius of a reference sphere.

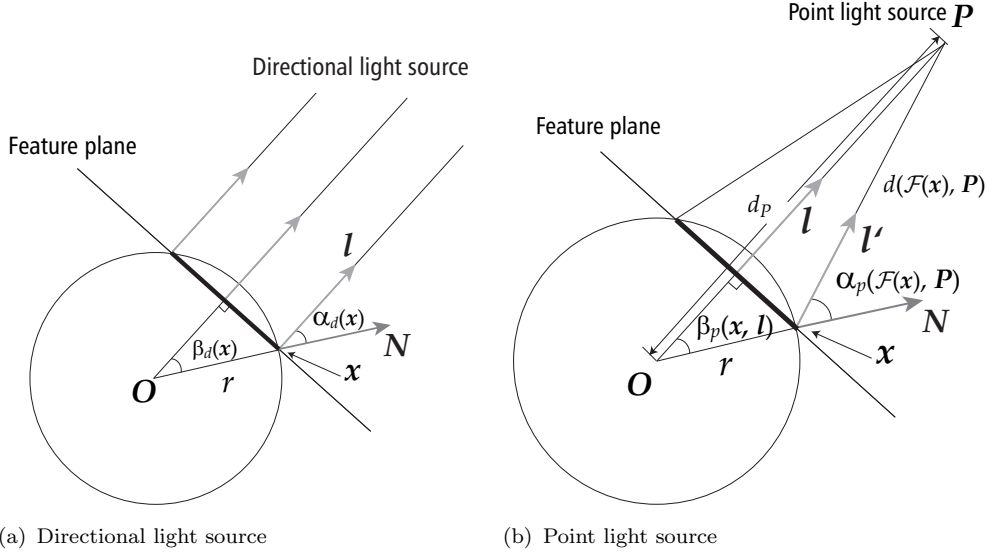


Fig. 5. Relation between a light source and a reference sphere

3.2.1 S_d -surface of Single Sphere

The bold line in Figure 5(a) illustrates a feature plane that is generated by a directional light source and a single sphere. Note that all the feature planes that are defined on an S_d -surface are parallel to each other, and a group of feature planes with different radiance characterizes the radiant intensity of a directional light source that illuminates the S_d -surface. Since the radiance of the group of feature planes varies according to $\beta_d(\mathbf{x})$, we describe the radiance with $\beta_d(\mathbf{x})$ instead of $\alpha_d(\mathbf{x})$. That is, the radiance, $I(\mathbf{x})$, at \mathbf{x} on an S_d -surface given by

$$I(\mathbf{x}) = \eta L_d \cos \alpha_d(\mathbf{x}) + \eta L_a \quad (9)$$

can be represented as

$$I(\mathbf{x}) = \eta L_d \cos \beta_d(\mathbf{x}) + \eta L_a, \quad (10)$$

where $\beta_d(\mathbf{x}) = \alpha_d(\mathbf{x})$. Selecting points on any three independent feature planes, we have the radiance ratio

$$\frac{I(\mathbf{x}_1) - I(\mathbf{x}_2)}{I(\mathbf{x}_1) - I(\mathbf{x}_3)} = \frac{I'(\mathbf{x}_1) - I'(\mathbf{x}_2)}{I'(\mathbf{x}_1) - I'(\mathbf{x}_3)} \quad (11)$$

where $I'(\mathbf{x}) = \cos \beta_d(\mathbf{x})$.

To summarize the analysis on S -surface, if the radiance ratio is given by Equation (11), we can deduce that the S -surface is an S_d -surface and thus obtain L_d and L_a from Equation (10).

3.2.2 S_p -surface of Single Sphere

Figure 5(b) shows the relation between a point light source and a single sphere. The radiance, $I(\mathbf{x})$, at \mathbf{x} on a feature plane is

$$I(\mathbf{x}) = \eta L_p \cos \alpha_p(\mathcal{F}(\mathbf{x}), \mathbf{P}) / d^2(\mathcal{F}(\mathbf{x}), \mathbf{P}) + \eta L_a, \quad (12)$$

where $\cos \alpha_p(\mathcal{F}(\mathbf{x}), \mathbf{P})$ and $d(\mathcal{F}(\mathbf{x}), \mathbf{P})$ can be formulated as

$$\cos \alpha_p(\mathcal{F}(\mathbf{x}), \mathbf{P}) = \frac{d_P^2 - r^2 - d^2(\mathcal{F}(\mathbf{x}), \mathbf{P})}{2rd(\mathcal{F}(\mathbf{x}), \mathbf{P})}, \quad (13)$$

$$d(\mathcal{F}(\mathbf{x}), \mathbf{P}) = \sqrt{d_P^2 + r^2 - 2rd_P \cos \beta_p(\mathbf{x}, \mathbf{l})}. \quad (14)$$

By substituting the above equations into Equation (12),

$$I(\mathbf{x}) = \eta L_p \frac{d_P \cos \beta_p(\mathbf{x}, \mathbf{l}) - r}{[d_P^2 + r^2 - 2rd_P \cos \beta_p(\mathbf{x}, \mathbf{l})]^{\frac{3}{2}}} + \eta L_a. \quad (15)$$

Equation (15) indicates that the radiance depends on unknown L_p , L_a , and d_P . However, the ambient light term can be eliminated by subtracting the radiance at points on any two feature planes. Besides, the lighting effect of the point light source due to L_p can also be canceled by selecting yet another point on any other feature plane and computing the radiance ratio,

$$\frac{I(\mathbf{x}_1) - I(\mathbf{x}_2)}{I(\mathbf{x}_1) - I(\mathbf{x}_3)} = \frac{I'(\mathbf{x}_1) - I'(\mathbf{x}_2)}{I'(\mathbf{x}_1) - I'(\mathbf{x}_3)} \quad (16)$$

where

$$I'(\mathbf{x}) = \frac{d_P \cos \beta_p(\mathbf{x}, \mathbf{l}) - r}{[d_P^2 + r^2 - 2rd_P \cos \beta_p(\mathbf{x}, \mathbf{l})]^{\frac{3}{2}}}.$$

Solving Equation (16), we could theoretically obtain d_P , and thereby L_p and L_a from Equation (15). Nevertheless, the solution to d_P is not indeed straightforward, which indicates the difficulty in estimating the point light sources solely by a single sphere.

3.2.3 S_p -surface of Difference Sphere

S -surface of a difference sphere has similar characteristics as does S_p -surface of a single sphere, except that the factor of ambient light, the second term of Equation (12), is precluded. Thus, radiance $I(\mathbf{x})$ at \mathbf{x} on a difference sphere is

$$I(\mathbf{x}) = \eta L_p^* \cos \alpha_p(\mathbf{x}, \mathbf{P}) / d^2(\mathcal{F}(\mathbf{x}), \mathbf{P}), \quad (17)$$

where L_p^* denotes the radiant intensity of a positive or negative point light source. Thus the radiance ratio is given by

$$\frac{I(\mathbf{x}_1)}{I(\mathbf{x}_2)} = \frac{I'(\mathbf{x}_1)}{I'(\mathbf{x}_2)} \quad (18)$$

where

$$I'(\mathbf{x}) = \frac{d_P \cos \beta_p(\mathbf{x}, \mathbf{l}) - r}{\left[d_P^2 + r^2 - 2rd_P \cos \beta_p(\mathbf{x}, \mathbf{l}) \right]^{\frac{3}{2}}}.$$

Expanding the equation about d_P , we obtain a polynomial of sixth degree of d_P , and then numerically solve it by Newton's and Bairstow's methods. It should be noted that it is much simpler to solve Equation (18) than to solve Equation (17) of single sphere in which the formulation hardly allows us to find a numerical solution.

4 Algorithm of Light Source Estimation

Based on the above discussions we propose a twofold algorithm for light source estimation as following:

step 0. Capture an image.

step 1. Generate an image of a difference sphere

step 1-1. Estimate parameters of point light sources

step 2. Update the input image by eliminating the lighting effects that is due to the estimated point light sources.

step 2-1. Estimate parameters of directional light sources and ambient light.

In each sub-step (1-1, 2-1), we estimate the parameters of light sources by an iterative operation. That is, we eliminate the effects of light source candidates one after another from the input image, and verify them by analyzing the residual in the image (see Figure 7). The procedure is:

- i. Convert each image region of the sphere to contour representation, and divide the contours into segments (see Section 4.1).
- ii. Extract candidates of S -surfaces, and analyze each candidate for estimating the corresponding light source (see Section 4.3).
- iii. Verify each of the light source candidates (see Section 4.4).
 - 1° Generate an image by eliminating the effect of the light source candidate from the input image.
 - 2° Analyze the residual radiance.

- If the surface has a uniform value, we regard the light source candidates that have been employed for the generation of the image as correct and terminate the procedure.
- If there exists a surface with negative values (*negative surface*), the light source candidate is judged to be incorrect.
- Otherwise, update the input image to what was generated by **iii-1°** and go to **i**.

4.1 Region Representation with Gray-Level Contour Segments

Since the contour representation reflects geometric characteristics of shading of objects while being robust against local noise, we consider that it is more suitable for extraction and analysis of S -surfaces than an ordinary image representation by an array of pixel values. The contour representation can be described as a geographic map where the radiance levels of pixels are regarded as height at corresponding locations [17].

As the surface of a sphere is illuminated by multiple light sources, the contour naturally consists of multiple segments, rather than looking like a simple arc. Thus, we divide every single contour line into contour segments in such a way that each segment represents an arc. Namely, we

- extract contours based on the shading of the sphere, and
- analyze the curvature of each contour and segment it into pieces at points where the curvature drastically changes. In practice, we compute the curvature at every pixel, λ , on each contour basically as the norm of the cross product of two vectors \mathbf{v}_F and \mathbf{v}_B : F and B are intersecting points of the contour and a circle which is centered at λ with a certain small radius (See Figure 6). For example, the norm is zero at a pixel on a straight part of a contour since the directions of the two vectors in this case are 180 degrees apart from each other.

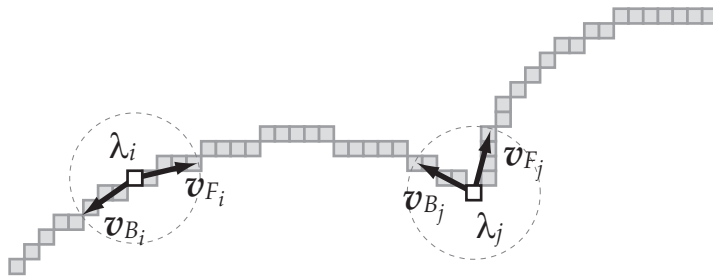


Fig. 6. Schematic diagram of computing curvature

The contour segmentation is an important process because it is the very clue with physical meanings for extracting an S -surface as a unit which we analyze

for estimating the corresponding light source.

4.2 Plane Estimation from a Contour Segment

After obtaining a contour segment, we estimate a plane in the 3D space to which the 2D points on the segment are projected. Since these 3D points may have some errors due to calibration or quantization of 2D image, we use RANSAC[26] for estimating a plane from the 3D points. The detail of the algorithm is as following:

1. Define a threshold, th , the number of iteration, T , and a ratio of points that are selected from a contour segment, μ .
2. For $t=1$ to T
 - Select m points ($m = \mu \times$ the number of points on the segment) at random and estimate a plane with them by using the least square method, and
 - Count a number of points whose distance to the estimated plane is within threshold, th .end For, and
3. Find the plane that has the maximum number of the consensus.

In practice, we use heuristically selected values for the parameters in step 1, that is, $th = 0.1 \times$ the radius of a sphere, $T = 100$, and $\mu = 0.5$.

4.3 Estimation of Light Source Candidates' Parameters

As we shown in the previous section, a contour segment on an S -surface forms an arc on a plane in 3D scene. Thus, in practice, we redefine it as **feature plane** (see Section 3.2). We extract the candidates of the S -surface using the gray-level contours in the following procedure.

- 1° For each contour segment, estimate a feature plane to which the segment fits most consistently.
- 2° Cluster the contour segments which indicate feature planes whose surface normals are in an identical or similar directions.
- 3° Represent a candidate of S -surface by the grouped contour segments.

For each candidate of S -surface we estimate the parameters of the light source using all the feature planes in the cluster by the method we have described in Section III. To be concrete, for each cluster of contour segments, we randomly select many pairs of feature planes and calculate the parameters of light source candidates by way of the radiance ratio which is given either by Equation (11)

or Equation (18).

In practice, when estimating point light sources in step 1-1, we first obtain a distribution of the estimate of d_P from which we compute the median, $\text{Med}(d_P)$, and the variance, $\text{Var}(d_P)$. We determine d_P by taking the average of the distances which are estimated as close to $\text{Med}(d_P)$, given $\text{Var}(d_P)$ is below a threshold. We then compute a distribution of L_p^* accordingly, and finalise the procedure by taking the median of it. The parameters are determined in this way so that the light source candidate appropriately illuminates the S -surface. If $\text{Var}(d_P)$ turned out to be above the threshold, however, we do not consider the cluster as derived from an S -surface but an M -surface.

4.4 Verification of Estimated Light Source Candidates

We verify the estimated light source candidates by analyzing images that are generated by eliminating their possible effects from the input image. That is, if the residual has negative values⁵, we can judge that the estimation was incorrect.

Suppose a reference sphere that is illuminated by three directional light sources (Figure 7). While there are four candidates of S -surface in the input image, correct S -surfaces are C_2 and C_4 , and the others are M -surfaces. Although it is not possible to identify S -surfaces among the candidates only by the iso-radiance contours, we can identify an M -surface by analyzing the residual that is generated by eliminating the effects of the light source candidates. That is, we can identify that C_3 is an M -surface since the *negative surface* appears in the third figure from the left in the first verification, which is generated by eliminating the effect of the light source candidate from C_3 . Continuing the procedure iteratively with the updated images, we find that three paths give the correct estimations. As these paths allow estimations of identical parameters of the same light sources, the lighting environment is correctly estimated.

For general lighting setting, as long as at least one correct S -surface exists, we can estimate the corresponding light source and continue the procedure by eliminating its effect from the input image accordingly.

As we described above, in our method we investigate all the possible paths, and determine the path that indicates the correct set of light sources. That is, it is a try-and-error approach in which an accumulation of errors or a selection of estimation paths is required in a global optimization. To obtain an optimal

⁵ In **step 1**, the residual should be zero. In **step 2**, the residual can also take a uniform value, which is regarded as the effect of ambient light.

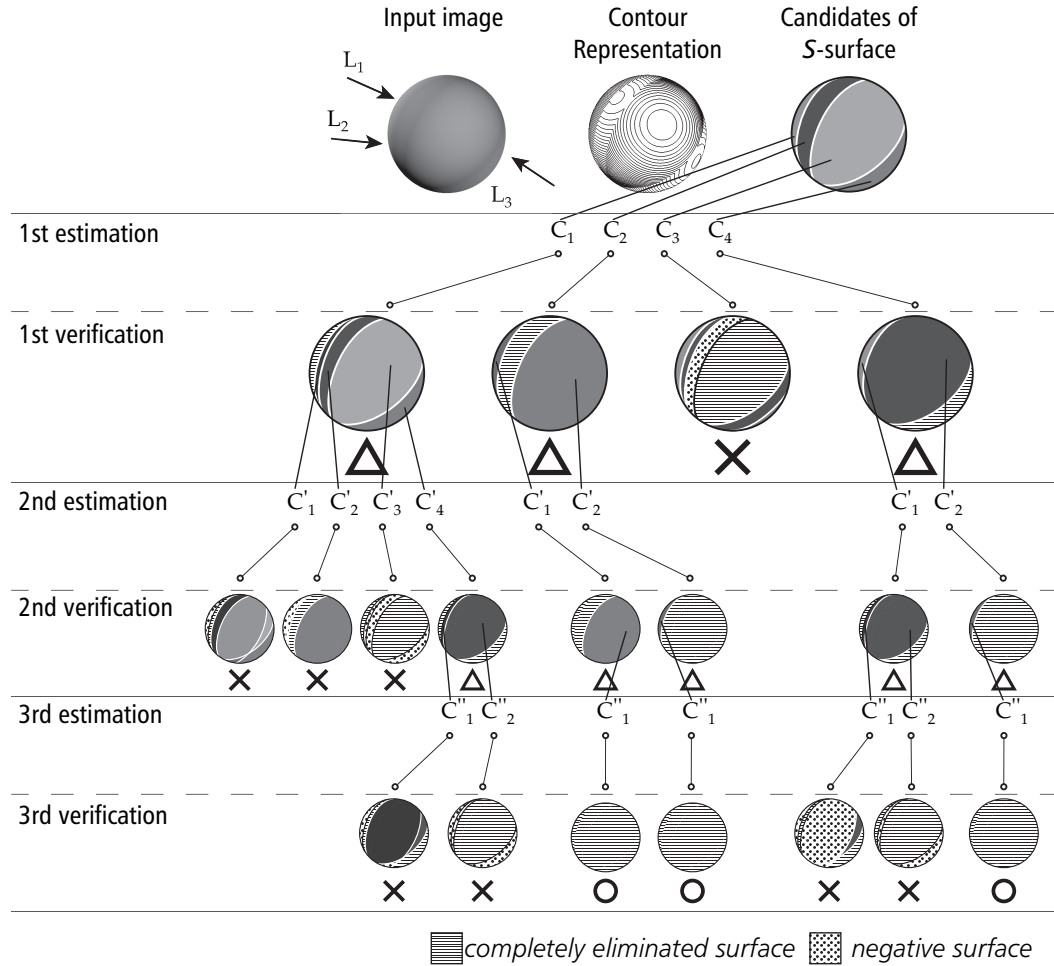


Fig. 7. An example of the estimation flow. ‘L’ denotes the light sources, and ‘C’ denotes S -surface candidates. \circ and \times signify correct and incorrect estimations, respectively, and \triangle an intermediate estimation.

set of the light sources, we evaluate all the combinations of estimated light sources in the successful paths.

5 Performance Evaluation

We demonstrate the effectiveness of our algorithm using a CG simulated scene and two cases of real scenes, one general case and the other by a setup like an open scanner, which we will later explain in Section 6.3. The lighting in one of the real scenes consists of three light sources, a point light source and two directional light sources. Estimating the parameters of them, we show the performance of our method by superimposing a virtual object in the scene with the photometric consistency. The other real scene is captured with the view to present the applicability of our method to an open scanner. We eliminate

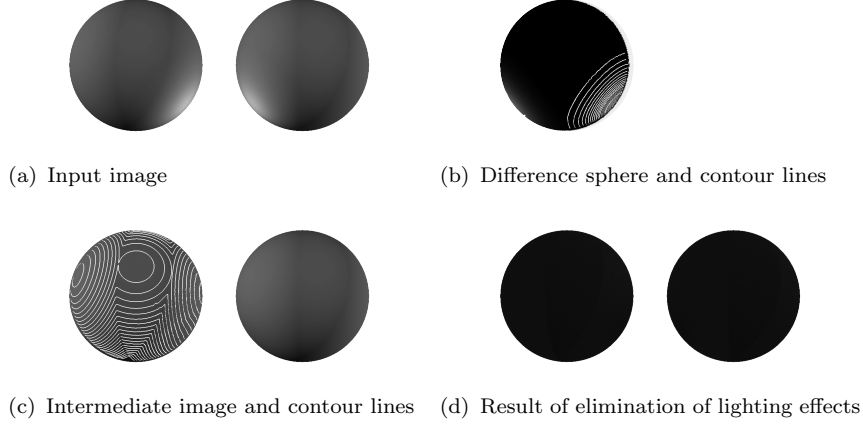


Fig. 8. Procedures of light source estimation. Intensity is emphasized in (b), and not all of the contour lines are shown in (c), (d), and (f) for display reason.

the non-uniform effect on a document that is placed on a desk by using the estimated parameters of a near light source in a complex lighting environment.

5.1 CG Simulation

Figure 8 exemplifies some results including the contour analysis on difference sphere. The input spheres are set to be illuminated by a point light source, two directional light sources, and ambient light. Each figure shows:

- (a) Input image.
- (b) Difference sphere generated from (a). Contour lines are superimposed.
- (c) Intermediate image — generated by eliminating the lighting effect by the estimated point light source from the input image. Contour lines are superimposed.
- (d) Result of elimination of lighting effects.

The intermediate image (c) shows the situation where the lighting effect by the point light source is eliminated and the remaining effect by directional light sources and ambient light is present. We then consider the image as a new input and estimate the parameters of light sources with the reference spheres which we regard as two reference spheres. (d) is a result of eliminating the effect by the light sources.

Table 1 shows the estimated parameters as the result. Light source 1 is best estimated whereas the accuracy tends to relatively decline as the estimation proceeds due to accumulation of errors. However, it can be seen that the overall performance is quite reasonable as the first trial of estimating both the positions and the radiant intensities of light sources.

Table 1

Estimated parameters of lighting environment in CG image

The estimation is for light source 1–3 and ambient light. The direction of directional light source is represented in (θ, ϕ) .

	Parameter	True	<i>Estimated</i>
Light source 1	Type	Point	<i>Point</i>
	Radiant intensity	200	<i>198.3</i>
	Position	(0.0, 2.0, -1.0)	<i>(-0.003, 1.97, -1.00)</i>
Light source 2	Type	Directional	<i>Directional</i>
	Radiant intensity	76	<i>72.4</i>
	Direction	(100.0, 0.0)	<i>(100.9, 1.92)</i>
Light source 3	Type	Directional	<i>Directional</i>
	Radiant intensity	85	<i>84.0</i>
	Direction	(120.0, -160.0)	<i>(121.1, -160.0)</i>
Ambient light	Radiant intensity	15	<i>15.1</i>

5.2 Real Scene – General Case

Figure 9 shows results of lighting environment estimation in a real scene. (a) shows an input image of a real scene which includes a point light source and two directional light sources, one roughly from the upper-right of the viewing direction and the other from the opposite side. Two reference spheres are placed on mounts whereas the point light source is located in between them and hidden by the frontal sphere. (b) shows a difference sphere, and the brighter pixels constitute a surface that is illuminated by a positive light source. Contour representation is also superimposed. (c) shows an image that is generated by eliminating the effect of the light source that is estimated in (b). Contour representation is also superimposed while denoting several S_d -surface candidates by the groups of contour lines. We verify these candidates by the *verification step* that is described in Section 4.4, and then obtain a correct set of light sources. Furthermore, (d) shows virtual spheres in the estimated lighting environment, and (e) shows the difference between (a) and (d). It illustrates that in the estimated lighting environment the virtual spheres are illuminated almost equivalently as in the input lighting environment.

Figure 10 illustrates a virtual object that is illuminated by estimated light sources. Images of (a), (b) and (c) are generated by illuminating a CG teapot by each of the estimated light source, respectively, whereas (d) is with all the three light sources and ambient light. (e) shows a synthesized image by adding the virtual object and the shadows in (d) into the real scene (f) that also was

Table 2

Estimated parameters of lighting environment in real scene

The estimation is for light source 1–3 and ambient light source. The direction of directional light source is represented in (θ, ϕ) . The origin is at the center of the bottom of the virtual teapot. X-axis and Y-axis are towards the right of the horizontal direction and the depth direction of the input image, respectively. Z-axis is orthogonal to the XY-plane.

	Parameter	<i>estimated</i>
Light source 1	Type	<i>Point</i>
	Radiant intensity	<i>4362848.9</i>
	Position	<i>(87.3, -139.7, 2.14)</i>
Light source 2	Type	<i>Directional</i>
	Radiant intensity	<i>102.7</i>
	Direction	<i>(62.3, -53.8)</i>
Light source 3	Type	<i>Directional</i>
	Radiant intensity	<i>129.5</i>
	Direction	<i>(51.1, 136.1)</i>
Light source 4	Type	<i>Ambient</i>
	Radiant intensity	<i>13.8</i>

shown in Figure 9 (a). The bulb as a point light source is now visible since the spheres have been removed while two little real dolls are placed for comparison. As the point light source is not completely isotropic and illuminates only the upper hemisphere from a certain height, the floor remains rather dark. Apart from that it illustrates that a CG object is added naturally with the real lighting environment.

Finally, we show the estimated light source positions and the radiant intensities of the real scene in Table 2.

5.3 Real Scene – Open Scanner

Figure 11 (a) shows the setup of an experiment for investigating the applicability of our method to an open scanner. The system is in a room where the lighting environment is complex, consisting of a large window, fluores-

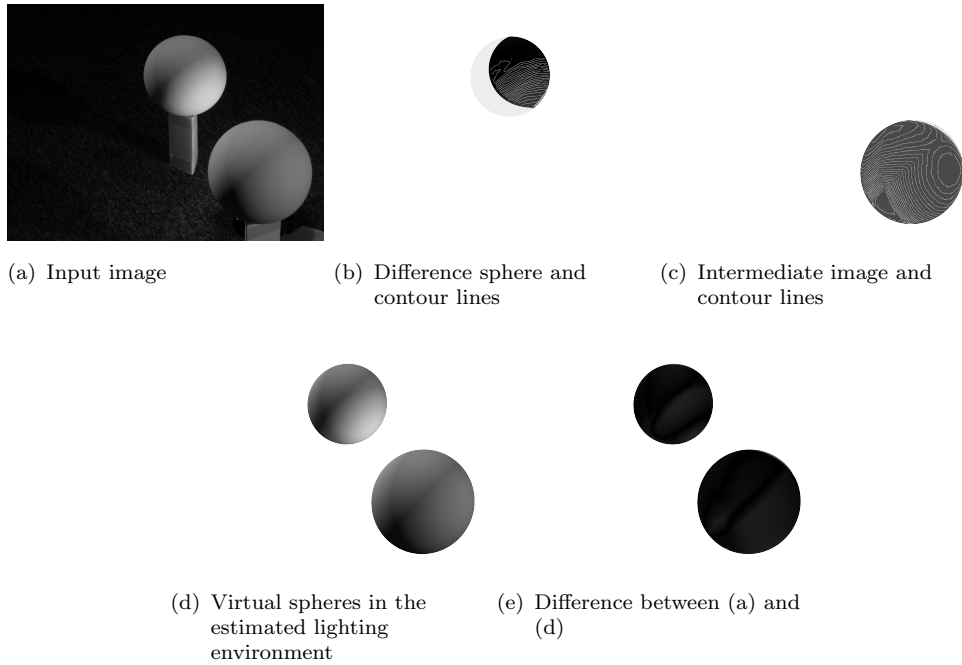


Fig. 9. Procedure of light source estimation (Real scene). Not all of the contour lines are shown in (b) and (c) for display reason.

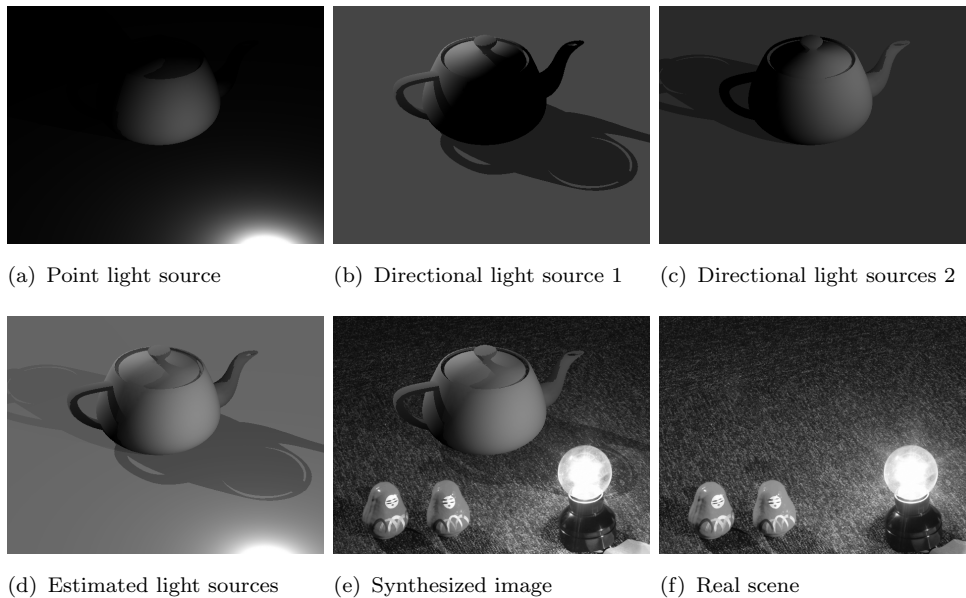


Fig. 10. The experiment of adding virtual object in a real scene. Images in (a), (b) and (c) are generated by illuminating a virtual object (teapot) by each estimated light source, respectively. (d) is generated with the above three light sources and ambient light, (e) is a synthesized image in (f).

cent tubes on the ceiling (not visible in the picture), and a desk lamp⁶. A

⁶ This is in contrast to the environment where only a desk lamp is assumed as seen for example in [24].

Table 3

Estimated parameters of a near point light source under complex lighting environment

The origin is at the center of the upper reference sphere. x-axis and y-axis are towards the right of the horizontal direction and the top of the vertical direction in the input image, respectively.

	Parameter	<i>estimated</i>
Light source 1	Type	<i>Point</i>
	Radiant intensity	<i>9107184.3</i>
	Position	<i>(8.3, -222.6, 184.1,)</i>

document on the desk is viewed by a camera mounted on the top, together with the two reference spheres (upper hemispheres) that are placed beside. (b) shows an example of captured image by the camera. Note that the surface of the document is illuminated non-uniformly due to the fact that the lamp is closely located. By using the two hemispheres imaged on both sides of the document, a difference sphere is generated as shown in (c). The influence of complex lighting has been eliminated in the difference sphere because it is regarded as a combination of directional light sources and ambient light. White lines in (d) shows the contour representation of the difference sphere. In particular, those which are judged to represent the S -surface derived from the near light source are shown separately in black. By using them we estimate the point light source, and list the resulting parameters in Table 3. In (e) we show a virtually computed document region with no texture that would be non-uniformly illuminated by the estimated nearby point light source. Finally, (f) shows an image which we generated by canceling the effect of the nearby light source by way of multiplying an brightness-negated image of (e) to the originally captured document image in (b). It can be observed that the inhomogeneously illuminated surface of the document appears as if it were under a uniform lighting.

The set of histograms in Figure 12 show the distributions of gray level intensities in the document regions of the captured and the enhanced images in Figure 11 (b) and (f), respectively. They illustrate that the enhanced image has a narrower distribution in the intensity range as the result of eliminating the effect of the near light source. To emphasize the result visually, in Figure 13 we show trimmed images of the document regions which we have generated by linearly stretching the lowest quarter to the full scale in the contrast of gray level intensities. Comparing the images in Figure 13, we see that the contrast of the image has been properly enhanced in (b) by the previously introduced simple processing whereas some area in (a) appears to be saturated. The result reflects that the parameters of the near light source have been successfully estimated in the complex lighting environment, and indicates the applicability of our method to an open scanner that requires to equalize nonuniform

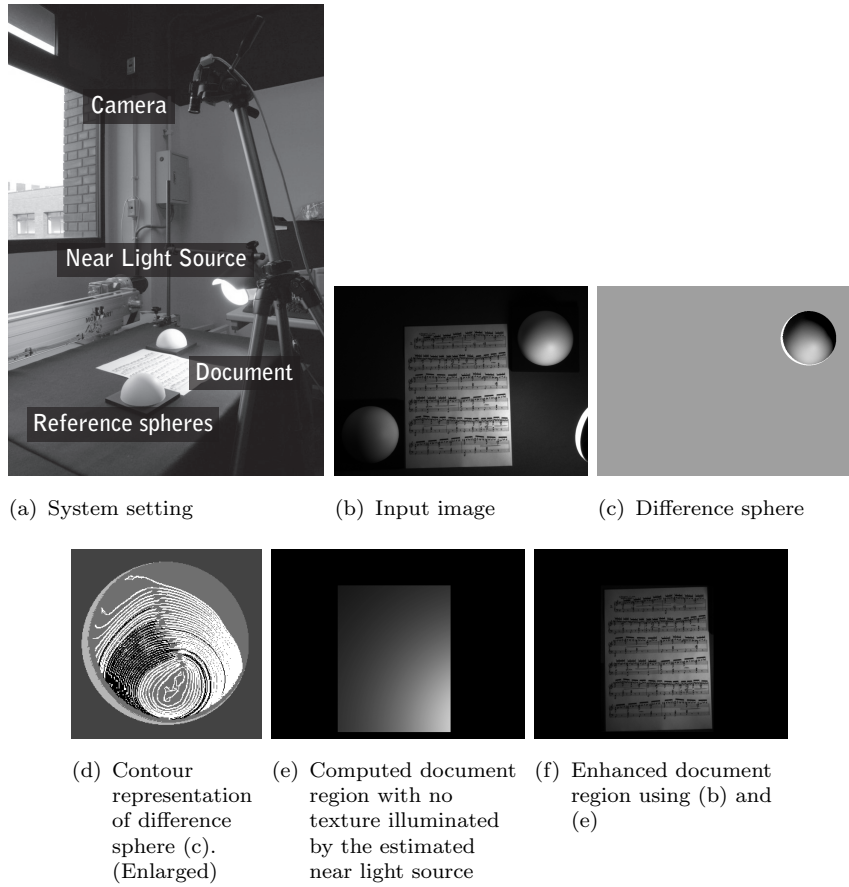


Fig. 11. Procedure of a near light source estimation under complex lighting environment for a use of an open scanner.

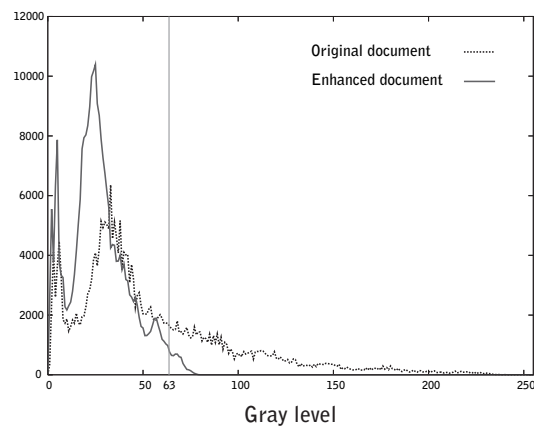


Fig. 12. Gray level histograms of document regions.

shading on a document which may be caused by a nearby light source.



(a) Captured document

(b) Enhanced document after eliminating the effect of the estimated near light source

Fig. 13. Document images. In both images the contrast of gray levels in the lowest quarter, $[0,63]$, has been linearly stretched to the full scale, $[0,255]$.

6 Discussions

In this paper, we have presented a novel technique for estimating parameters of near point light sources as well as directional light sources and ambient light. We have mainly concerned ourselves with indoor scene where the direct near light sources are more dominant compared to indirect reflection. We employ a contour representation of an image for analyzing shading of a pair of reference spheres and characterize 3D geometric and photometric properties of the light sources. In particular, we have proposed the difference sphere which enables us to estimate parameters of point light sources by eliminating the lighting effects of ambient light and directional light sources. In order to show the theoretical availability, we have demonstrated the effectiveness by applying our method to a CG image, which is generated with a point light source, two directional light sources, and ambient light. Applying our method also to a real scene, we have illustrated the validity by synthesizing a virtual object in the scene in a geometrically and photometrically consistent manner. Although we have mainly focused on the theoretical aspects of light source estimation, our belief is that the concepts presented here have also practical applications in indoor scene. In fact, we have also examined our method using a setup like an open scanner, and shown the possibility to equalize the influence of nearby light source on a document. Despite the analyses which we have made so far, there remains some extensions and open issues which we discuss below.

6.1 Relationship between Size of a Reference Sphere and Distance between the Sphere and a Near Point Light Source

In the case of practical estimations, the range in which the point light sources can be identified depends on the size of the reference sphere and the distance between the light source and the sphere. That is, a light source that is positioned at a longer distance from the reference sphere can be regarded as a directional light source.

Figure 14(a) illustrates a reference sphere that is illuminated by a point light source, where \mathbf{O} and \mathbf{P} denote positions of the reference sphere and the point light source, respectively. The positions, \mathbf{x}_p and \mathbf{x}_d , denote the farthest points illuminated by the point light source and the directional light source that have the identical direction, \mathbf{l} , respectively. Note that \mathbf{O} , \mathbf{P} , \mathbf{x}_p and \mathbf{x}_d are aligned on an identical plane. The arc length, $l_{\mathbf{x}_p, \mathbf{x}_d}$, between \mathbf{x}_p and \mathbf{x}_d is given by

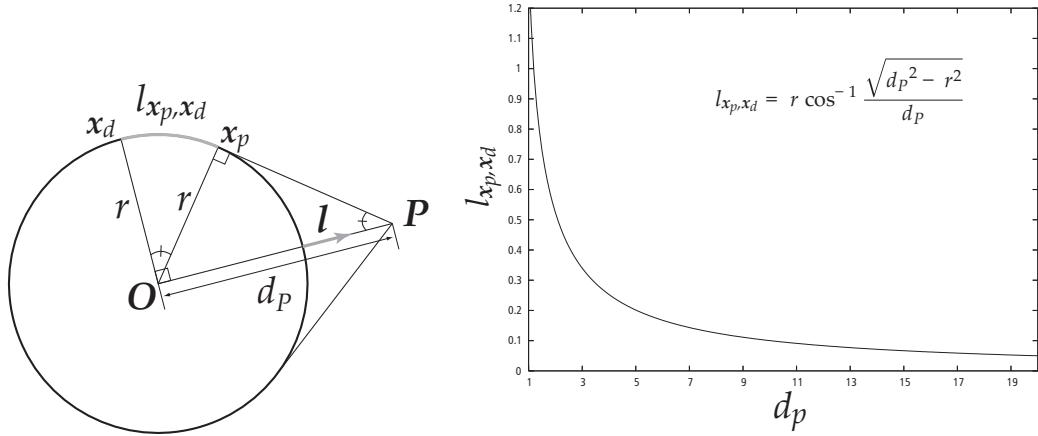
$$l_{\mathbf{x}_p, \mathbf{x}_d} = r \cos^{-1} \frac{\sqrt{d_p^2 - r^2}}{d_p}, \quad (19)$$

where d_p denotes the distance between \mathbf{O} and \mathbf{P} , and r the radius of the reference sphere. By analyzing $l_{\mathbf{x}_p, \mathbf{x}_d}$ according to d_p and r , we can determine the range in which we identify a point light source with a reference sphere.

Figure 14(b) illustrates the relationship between the length, $l_{\mathbf{x}_p, \mathbf{x}_d}$, and the radius, r , of a reference sphere in the case that the reference sphere has the radius of the size of 1. The figure indicates that $l_{\mathbf{x}_p, \mathbf{x}_d}$ becomes 0.1 at about ten of d_p . Namely, the figure can be regarded as an index for designing size and positions of reference spheres for creating the difference sphere, position of camera, resolution of captured images, and so on. Therefore we can configure a setting of our method for estimating a complex lighting environment by considering the relationship between reference spheres and light sources.

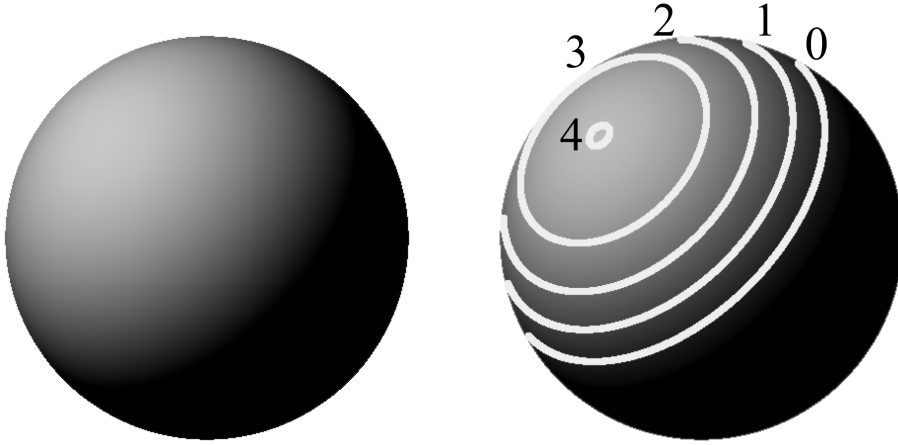
6.2 Robustness of Plane Estimation from a Contour Line

In this section, we evaluate the robustness of our plane estimation algorithm from a contour line by a CG simulation. We first evaluate how sensitive our algorithm is to calibration errors, and then how the accuracy of plane estimation varies by a length of a contour line. For the evaluation, we create an image with a single sphere and a single directional light source, and extract several contour lines from the image (Figures 15(a) and 15(b)). In Figure 15(b), we enhance the lines whose radiances are 40, 80, 120, 160 and 200, which we used for evaluation, and the lengths of the lines are 447, 457, 461, 524 and 58 pixels, respectively.



(a) Reference sphere illuminated by a near point light source (b) Relation between l_{x_p, x_d} and d_p ($r = 1$)

Fig. 14. Relation between a reference sphere and a point light source



(a) Input image

(b) Extracted contour lines

Fig. 15. CG image and extracted contour lines for evaluation

The procedure for evaluating the sensitiveness is shown in the following:

- (1) Estimate planes from the contour lines by adding noise to the 3D points that are computed from the contour lines as

$$\mathbf{X}_i = f(\boldsymbol{\lambda}_i) + \mathcal{N}, \quad (20)$$

where \mathbf{X}_i denotes 3D position of $\boldsymbol{\lambda}_i$ on a contour line, which is computed by f . \mathcal{N} denotes added noise which is given by

$$\mathcal{N} = \epsilon r \mathbf{V}, \quad (21)$$

where r denotes the radius of the sphere, \mathbf{V} a random 3D vector whose length equals 1, and ϵ a noise coefficient.

- (2) Compute the dot product between the direction of the light source and

the normal of the estimated plane with $0 \leq \epsilon \leq 1$.

Furthermore, the procedure for evaluating the accuracy of plane estimation depending on the length of a contour line is shown in the following:

- (1) Shorten the length of a contour line by 1 pixel from the end.
- (2) Estimate the plane with the line, and compute the dot product between the direction of the light source and the normal of the estimated plane.
- (3) Repeat this procedure until the length becomes zero.

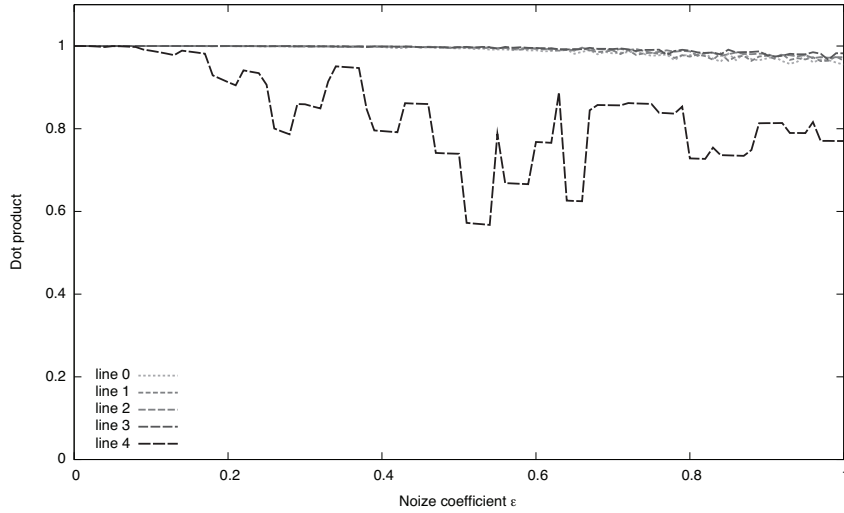
Figures 16(a) and 16(b) show the results of the evaluations. As shown in Figure 16(a), our method shows robustness against errors of 3D positions of contour lines. Only Line 4 involves instability because its length is much shorter than those of the other three lines. Figure 16(b) illustrates of the accuracy of plane estimation depending on the length of the last 100 pixels of each line. As we can see, Line 4 shows high stability in spite of its short length. These results tell us that we need to find longer and almost-ellipsoid contour lines for robust plane estimation.

One of the future work motivated by this result will be to increase the reliability to contour lines which are estimated from its length and degree of ellipsoid, and estimate a feature plane with reliable contour lines.

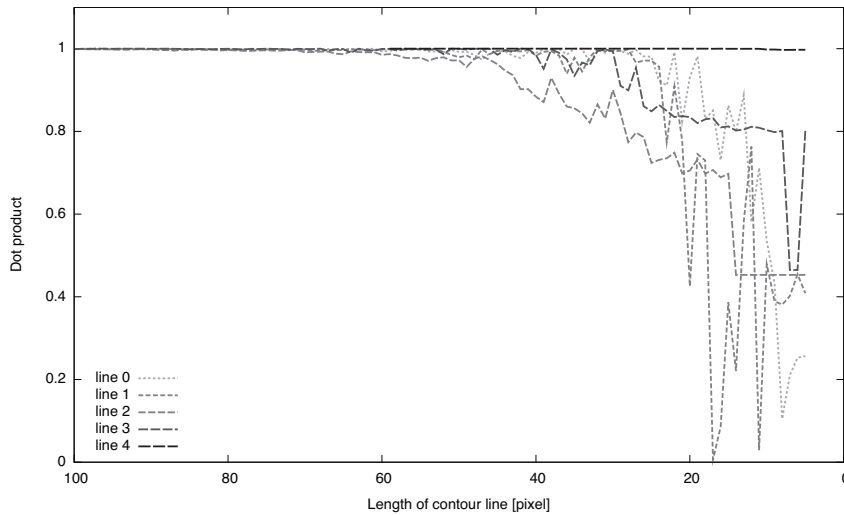
6.3 *Application to Open Scanner*

As we have already seen, we consider our technique suitable to indoor scene where an actual light sources include those located nearby. We consider that direct applications of the method include "open scanner", an office equipment. An open scanner, OCR by digital camera in other words, is used for example in a bank office where a large number of documents need be scanned speedily. The advantage of it is that the process of scanning a document is drastically facilitated without the need for opening and closing the cover. However, as it does not have a cover, open surface of the document being scanned must be illuminated by a uniform light source, which is often difficult in an office environment where desk lamps are placed nearby the scanner.

One of the motivations of the proposed technique in the viewpoint of practical applications is to deal with such a situation so that an open scanner becomes available even for scanned surface that is illuminated non-uniformly. We envision that a pair of spheres as the probe would be mounted as parts of the equipment in such a way that they are visible to the (high-resolution) digital camera whose primary role is to scan documents. Hence, a single camera can be used for dual purposes, scanning documents and estimating the parameters of nearby light sources (and thereby equalizing the influence of them). It



(a) Calibration errors



(b) Length of contour lines

Fig. 16. Evaluation of robustness of plane estimation.

should also be noted that the estimation of radiant intensity is then essential in such an application.

6.4 Future work

Although we have described our algorithm as a general framework, our practical investigation has so far been limited to the case of estimating a small number of major light sources in a scene. As a future work, first we would like to examine our method in an environment with a larger number of light sources which would make the identification of S -surface(s) complicated. In order to handle the challenging situation, however, it should be useful to consider critical points for region segmentation, as discussed in [18]. Another

aspect that we wish to investigate is the availability of Lambertian reflectance model for estimation of complex lighting environment. Since the Lambertian reflectance model performs low-pass filtering of the lighting environment [19–21], the problem may be ill-posed or numerically ill-conditioned. For the problem to be alleviated, we need to consider the configuration of reference spheres for effectively generating the difference sphere. In particular, we would like to study the possibility to incorporate the model for computing the accuracy of low-dimensional harmonic representations under near lighting that was recently derived by Frolova et al. [22] almost at the same time as the initial publication of this work [23].

Acknowledgements

This work is supported by MEXT, Japan, under a Grant-in-Aid for Scientific Research (No. 13224051 and No. 16680010), and in part by national project on “Development of high fidelity digitisation software for large-scale and intangible cultural assets.” We wish to thank the anonymous reviewers for their invaluable comments.

References

- [1] B.K.P. Horn. Image intensity understanding. *Artificial Intelligence*, Volume 8, pp. 201–231, 1977.
- [2] A. P. Pentland. Finding the illumination direction. *Journal of Optical Society of America*, 72(4):448–455, 1982.
- [3] Q. Zheng and E. Chellappa. Estimation of illuminant direction, albedo, and shape from shading. *IEEE Transactions on Pattern Analysis and Machine Intelligence*, 13(7):680–702, 1991.
- [4] D. R. Hougen and N. Ahuja. Estimation of the light source distribution and its use in integrated shape recovery from stereo and shading. *4th IEEE International Conference on Computer Vision*, pages 148–155, 1993.
- [5] S. R. Marschner and D. P. Greenberg. Inverse lighting for photography. In *Fifth Color Imaging Conference*, pages 262–265, 1997.
- [6] Y. Yang and A. Yuille. Sources from shading. In *IEEE Conference on Computer Vision and Pattern Recognition*, pages 534–539, 1991.
- [7] Y. Zhang and Y. Yang. Multiple illuminant direction detection with application to image system. *IEEE Transactions on Pattern Analysis and Machine Intelligence*, 23:915–920, 2001.

- [8] W. Zhou and C. Kambhamettu. Estimation of illuminant direction and intensity of multiple light sources. In *European Conference on Computer Vision*, pages 206–220, 2002.
- [9] A. Maki: Estimation of Illuminant Direction and Surface Reconstruction by Geotensity Constraint. *Pattern Recognition Letters*, Volume 21:13–14, pages 1115–1123, 2000.
- [10] D. Miyazaki, R.T. Tan, K. Hara, and K. Ikeuchi. Polarization-based Inverse Rendering from a Single View. In *IEEE International Conference on Computer Vision*, pages 982–987, 2003.
- [11] K. Hara, K. Nishino, and K. Ikeuchi. Multiple Light Sources and Reflectance Property Estimation Based on a Mixture of Spherical Distributions. In *IEEE International Conference on Computer Vision*, pages 1627–1634, 2005.
- [12] P. Debevec. Rendering synthetic objects into real scenes: Bridging traditional and image-based graphics with global illumination and high dynamic range photography. In *ACM SIGGRAPH*, pages 189–198, 1998.
- [13] I. Sato, Y. Sato, and K. Ikeuchi. Acquiring a radiance distribution to superimpose virtual objects onto a real scene. *IEEE Transactions on Visualization and Computer Graphics*, 5(1):1–12, 1999.
- [14] I. Sato, Y. Sato, and K. Ikeuchi: Illumination distribution from shadows. *IEEE Transactions on Pattern Analysis and Machine Intelligence*, 25(3):290–300, 2003.
- [15] M. W. Powell, S. Sarkar, and D. Goldgof. A simple strategy for calibrating the geometry of light sources. *IEEE Transactions on Pattern Analysis and Machine Intelligence*, pages 1022–1027, 2001.
- [16] W. Zhou and C. Kambhamettu. Estimation of the size and location of multiple area light sources. In *IAPR International Conference on Pattern Recognition*, pages 214–217, 2004.
- [17] T. Asano and S. Kimura. Contour representation of an image with applications. In *IPSJ Signotes Algorithms*, number 058-009, pages 65–70, 1997.
- [18] Y. Wang and D. Samaras. Estimation of multiple illuminants from a single image of arbitrary known geometry. In *European Conference on Computer Vision*, pages 272–288, 2002.
- [19] R. Ramamoorthi and P. Hanrahan. A signal-processing framework for inverse rendering. In *ACM SIGGRAPH*, pages 117–128, 2001.
- [20] R. Basri and D. W. Jacobs. Lambertian reflectance and linear subspaces. *IEEE Transactions on Pattern Analysis and Machine Intelligence*, 25(2):281–233, 2003.
- [21] P. Nillius and J.-O. Eklundh. Automatic estimation of the projected light source direction. In *IEEE Conference on Computer Vision and Pattern Recognition*, volume I, pages 1076–1083, 2001.

- [22] D. Frolova, D. Simakov and R. Basri. Accuracy of Spherical Harmonic Approximations for Images of Lambertian Objects under Far and Near Lighting. In *European Conference on Computer Vision*, pages 574–587, 2004.
- [23] T. Takai, K. Niinuma, A. Maki and T. Matsuyama. Difference Sphere: An Approach to Near Light Source Estimation. In *IEEE Conference on Computer Vision and Pattern Recognition*, Volume I, pp. 98–105, 2004.
- [24] J. Bouguet and P. Perona. 3D Photography on Your Desk. In *IEEE International Conference on Computer Vision*, pages 43–50, 1998.
- [25] X. Cao and H. Foroosh. Camera Calibration and Light Source Orientation from Solar Shadows. *Computer Vision and Image Understanding*, Volume 105, Issue 1, pages 60–72, 2007.
- [26] M. A. Fischler and R. C. Bolles. Random sample consensus: a paradigm for model fitting with applications to image analysis and automated cartography. *Communications of the ACM*, Volume 24, Issue 6, pages 381–395, 1981.